STM JOURNALS

Journal of
Polymer & Composites

https://journals.stmjournals.com/jopc

ISSN: 2321-2810 (Online)
ISSN: 2321-8525 (Print)
Volume 14, Special Issue 3, 2026
DOI (Journal): 10.37591/JoPC

Research JoPC

Mathematical Modelling and Experimental Analysis of a 3D Printed PLA UAV Propeller using NACA 4412 Airfoil

Mubina[1,*], Sushila Rani[2]

Abstract

The usage of unmanned aerial vehicles (UAVs) has grown significantly because they are cost-effective and easy to availability for many applications. However, researchers have focused on the designing for various UAV propeller/rotors geometries, including their aerodynamic performance and structural examination. An elegant, designed propeller can enhance the UAV's endurance limit and its reliability. This research focuses on designing of UAV propeller and its fabrication using Polylactic acid (PLA) material using bamboo X1 carbon 3D printing machine for the evaluation of UAV propellers and evaluating their aerodynamic and aeroacoustics properties. It examines the thrust in Newton, and sound power level (SPL) in dB of a simple plane propeller based on the NACA 4412 air foil. Here, the authors developed a new approach for the designing of UAV propeller using a mathematical model. The experimental results obtained from using test-rig for the 3D-printed PLA propeller to obtained insights into the effectiveness of this method for creating lightweight, well-organized, and noise-conscious UAV components. This research work focused on the potential of a NACA 4412 air foil-based 3D printed UAV propeller for its aerodynamic and aeroacoustics performance.

Keywords: UAV propellers, acoustic, aerodynamic, PLA, 3D printing

INTRODUCTION

Unmanned aerial vehicles (UAVs) are basically used for its potential applications and easy to operate. It has various applications in general purposes like entertainment, photography, videography, product delivery and in military and civilian domains. It has attained unexpected success in surveillance and monitoring, firefighting, wildlife photography, rescue operations, and other areas too [1, 2]. The miscellaneous range of applications for UAVs commands the selection of specific types based on their intended use. The types of UAVs are influenced mainly by their payload capacity, which in turn determines their total weight range. This manuscript aims to study UAVs, and the features involved their behaviour. Prior to selection of components like UAV Frame, batteries, propellers, and motors, it is vital to have a thorough understanding of the UAVs total weight range. UAVs are categorized based on their payload capacity and altitude range, which significantly influence their design and operating condition. These categories include large drones weighing more than 600 kg, with the ability of operating above 150 km Mean Sea Level (MSL), as well as smaller variants: small drones (20–150 kg), mini drones (2–20 kg), micro drones (200 grams to 2 kg), and nano drones (up to 200 grams). Each category is focused for specific elevation restrictions: small drones, mini drones, micro drones and nano drones are limited below 150 km, 40 km, 25 km, and 5 km respectively [3, 4]. Several experiments have been performed to enhance the endurance limit/battery life of the UAVs. Several investigators are focused on propellers' shape for small unmanned aerial vehicles, to enhance the thrust generation and propeller behavior in low

***Author for Correspondence**
Mubina

[1,*]Research Scholar, Department of Mechanical Engineering, Delhi Technological University, Delhi, India
[2]Associate Professor, Department of Mechanical Engineering, Delhi Technological University, Delhi, India

Received Date: September 09, 2025
Accepted Date: January 13, 2026
Published Date: May 25, 2026

Citation: Mubina, Sushila Rani. Mathematical Modelling and Experimental Analysis of a 3D Printed PLA UAV Propeller using NACA 4412 Airfoil. Journal of Polymer & Composites. 2026; 14(Special Issue 3): S825–S832p.

Reynolds flow conditions [5, 6].

The traditional NACA airfoil with high Reynold's number has been used for the larger aircraft. Therefore, to achieve optimal aerodynamic performance, a low Reynolds number air foil is recommended for small UAVs. Generally, a low Reynolds number airfoil has been used on small aircraft to achieve a maximum lift-to-drag ratio [7]. Researchers examined the aerodynamic efficacy of a UAV propeller using the NACA 4412 airfoil. Essentially, numerical simulations are necessary to investigate velocity and pressure fields, pressure coefficients, and lift forces. The researchers selected the NACA 4412 profile as optimal for propeller design to mitigate the noise and enhance the thrust [8, 9]. In small-scale rotary-wing UAVs, an aeroacoustics measurement is performed on an isolated rotor-airframe configurations. It was successfully applied to a CFD-based numerical simulation for aeroacoustics predictions for selected configurations [10]. Limited research is available in shape modification to reduce the noise.

Despite extensive studies on UAV propeller performance, most previous works have focused on either numerical simulations or experimental analyses in isolation. There is a lack of comprehensive studies that combine both approaches to evaluate the aerodynamic and aeroacoustic performance of 3D-printed propellers. This gap is particularly significant for UAVs operating in indoor environments, where thrust efficiency and noise reduction are critical. In this study, we address this gap by conducting mathematical modeling, fabrication, and experimental analyses on PLA-based propellers to assess their aerodynamic and aeroacoustic performance. This provides a thorough evaluation of thrust generation and noise characteristics, offering insights into optimal propeller design for quieter and more efficient UAV operation [11–13]. Several factors influenced the operation of the UAV propellers, including air density, propeller blade size, and blade pitch. These factors play a crucial role in defining the aerodynamic and aeroacoustics characteristics of the UAV propellers, which in turn affect the overall efficiency and operational noise of UAVs. This research focuses on the experimental analysis of the aerodynamic performance, including thrust analysis and aeroacoustics properties (sound pressure level), of the NACA 4412 airfoil-based UAV propeller, a widely used design in UAV applications. The NACA 4412 airfoil is selected for its low Reynolds number, which provides maximum lift and stall resistance [14–15]. The authors developed a comprehensive mathematical model of a NACA 4412 Airfoil 7×2.3 propeller, focusing on its geometric parameter analysis. Furthermore, it is fabricated using additive manufacturing, specifically a BAMBOO 3D FDM printer.

The structure of the paper is as follows: Section II represents a detailed description of the propeller's design and mathematical modeling process. Section III presents the low-fidelity testing (experimentation) methodology used to observe thrust and noise characteristics. Section IV presents the findings related to acoustic and thrust performance, accompanied by a detailed discussion of the results. Finally, Section V concludes the study presented in this research.

MODELLING OF THE PROPELLER

In this research, the authors selected a low Reynolds number 7×2.3 Propeller for aerodynamic and aeroacoustic analysis as shown in Figure 1. To increase the precision of the study, each blade has sixteen sections (slices), giving a total of thirty-two sections for the complete propeller, as illustrated in Figure 2. The chord length and blade angle for each portion may be precisely controlled thanks to this segmentation. The propeller models are made using methods that define key parameters, including tip speed ratio (TSR), airflow angle, and blade angle [8]. This method confirms a detailed and accurate illustration of the propeller's geometry and aerodynamic characteristics. The Geometrical limitations of the NACA 4412 airfoil 7×2.3, 3D Printed Propeller are tabulated in Table 1. Figure 3 shows plots of Tip Speed Ratio (TSR) and Angle of Attack (AOA) vs. non-dimensional radial location (D/d), alongside chord length (c) and blade angle variations for a propeller using the NACA 4412 airfoil. This analysis optimizes propeller performance by identifying ideal operating conditions, ensuring structural integrity, and enhancing efficiency. This approach enables the development of high-performance propellers that strike a balance between efficiency and adaptability.

Figure 1. 3D CAD model of 7” NACA 4412 air foil propeller.

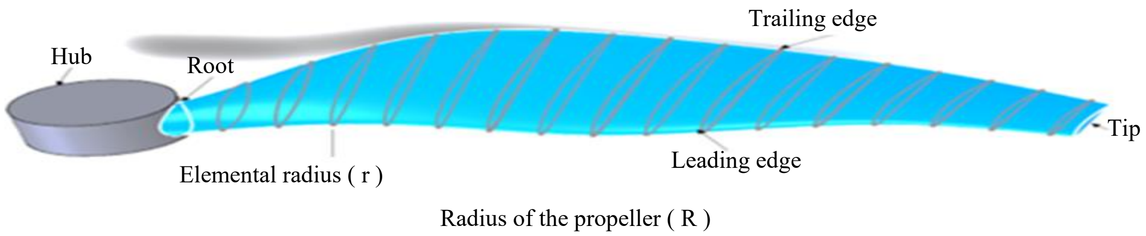

Figure 2. Nomenclature of a propeller.

Data Reduction

The following are the mathematical formulas for the design of an efficient UAV propeller:

Tip speed ratio (TSR) (λ), It is defined as the tangential speed of the propeller blade tip divided by the air velocity is known as the tip speed ratio (λ). An increase in tip speed may cause the propeller system to vibrate more and produce more noise.

$$\lambda = \frac{r.\omega}{v} \tag{1}$$

Here, ω is the angular speed [rad/s] of the propeller, v is the air velocity [m/s], r is the radius at the computation point [m], and R is the radius at the tip [m].

*Chord Length (*c) is the distance from its leading edge to the trailing edge. A longer chord length can enhance the efficiency of the rotor by providing a larger surface area for air interaction. This increased width allows the propeller to generate maximum lift and thrust, thereby improving overall performance.

$$c = \frac{5.6.\,R^2}{2.r\,.C_l.\lambda^2} \tag{2}$$

Here, R is the propeller radius, r is the distance from the centre to the calculation point, C_l is the lift coefficient and λ is the Tip speed ratio (TSR).

This mathematical formula comes from Betz's optimal circulation theory and Prandtl's tip loss corrections. It helps to determine the ideal chord length (c) at any radial position along a propeller blade to achieve maximum aerodynamic efficacy. This formula is widely used in the preliminary design of wind turbine and propeller blades, though practical designs often require modifications to account for structural and manufacturing constraints.

The angle of attack (α) is the angle between an airfoil’s chord line and the incoming airflow. This crucial parameter affects the propeller blade's performance by influencing lift, drag, and overall efficiency. Finding the right angle is essential - too small an angle won't generate enough lift, while too large an angle risks stalling. The optimal angle maximizes the blade's performance.

Inflow Angle (φ), The inflow angle (φ) represents the angle formed by the direction of the entering wind and the propeller's rotational axis.

$$\varphi = \tan^{-1}\frac{2}{3\,\lambda} \tag{3}$$

Blade Angle (β) is a fundamental parameter in propeller design that represents the angle between the rotational plane (reference plane) and the chord line of the blade section. The blade angle varies along the radius and directly impacts lift and thrust generation. It can be expressed mathematically as:

$$\beta = \alpha + \varphi \tag{4}$$

Working together with the chord length formula shown, it must be optimized for maximum propeller efficiency. Some designs allow angle adjustments to maintain optimal performance under varying conditions.

Advance ratio (J) is a dimensionless number that describes the relationship between an aircraft's forward speed and its propeller's rotational speed. It is calculated using the formula:

$$J = \frac{V}{n.D} \tag{5}$$

Here, V is the Forward velocity (in m/s), n is the propeller's rotational speed in rotation per second and D is the propeller's diameter (in m).

Efficiency of the Propeller (ɳ) is typically expressed as the proportion of output power (thrust power) to input power (shaft power). The formula for propeller efficiency is:

$$\eta = (F_t.V)/P \text{ or } \frac{J\,C_t}{C_p} \tag{6}$$

Here, F_t is thrust (Newton), V is the Forward velocity (in m/s), P is the input power in (Watt), C_t and $C_p$is the thrust coefficient and the power coefficient, respectively.

Blade-Element Theory (BET) is a classical method used to estimate propeller performance by dividing the blade into small radial segments and analyzing the aerodynamic forces on each [16–17]. The relative velocity at a radial station depends on the freestream velocity and the rotational speed, while the inflow angle determines the local angle of attack.

The elemental thrust generated by a blade section of chord $c(r)$ at radius r is given by:

$$dT = B * \frac{1}{2}\rho V_{\text{rel}}^2 c(r)[C_L \cos\phi - C_D \sin\phi]dr \tag{7}$$

Here, dT represents the elemental thrust generated by a blade segment, while B is the total number of blades. The term ρ denotes the air density, and Vrel is the relative velocity of the airflow at the blade element. The chord length at a given radial position is represented by c(r), and dr is an infinitesimal length along the blade radius. The coefficients C_L and C_D correspond to the lift and drag of the airfoil section, respectively, and ϕ\phiϕ is the inflow angle, defined as the angle between the relative airflow and the plane of rotation. This formulation enables the calculation of the thrust contribution from each blade element by accounting for the aerodynamic forces acting along and perpendicular to the blade.

LOW FIDELITY TEST FOR THRUST AND ACOUSTIC ANALYSIS

A low-fidelity test was conducted to evaluate the thrust performance and acoustic characteristics of the 3D-printed propeller. This propeller is fabricated using a Bamboo X1 carbon 3D printer with PLA material. Polylactic Acid (PLA) is a biodegradable polymer that offers good mechanical strength and environmental sustainability, making it highly suitable for manufacturing new components through 3D printing. It is an economical and sustainable material for 3D printing, chosen due to its ease of fabrication using FDM 3D printing, good dimensional stability, adequate stiffness-to-weight ratio, and cost-effectiveness for the rapid prototyping of small UAV propellers [18, 19]. This introductory testing method provides a cost-effective and effective way to gather initial performance data.

This experimental test rig is assembled with the following components: a brushless DC motor

Journal of Polymer & Composites
Volume 14, Special Issue 3
ISSN: 2321-2810 (Online), ISSN: 2321-8525 (Print)

(BLDC) mounted on an F-450 3D-printed quadcopter arm, an RC transmitter, and a LiPo battery, all controlled by an Electronic Speed Controller (ESC). Thrust is measured using a weighing scale with a 10 kg capacity, while acoustic data is captured by using a CESVA SC-260 sound level meter [20] for precise performance evaluation. This setup permits a comprehensive evaluation of the rotor's performance, including thrust and acoustic performance. This experimental setup provides a crucial standard for understanding the initial aerodynamic and acoustic behavior of the propeller evaluations.

Table 1. Geometrical parameter of the NACA 4412 Airfoil 7×2.3, 3 D printed propeller.

S.N.	D/d	TSR (λ)	Angle of Attack *(α)*	Inflow Angle *(φ)*	Blade Angle *(β)*	Chord Length *(c)*
1	3.116725	3604.72	25.9	1.570380206	27.47038021	17.21
2	2.654303	4232.72	23.2	1.570441945	24.77044194	19.96
3	2.31137	4860.72	20.59	1.570487731	22.16048773	21.89
4	2.046911	5488.72	15.5	1.570523039	17.07052304	23.2
5	1.836756	6116.72	13.94	1.570551097	15.5105511	23.96
6	1.665736	6744.72	12.69	1.570573931	14.26057393	24.07
7	1.52385	7372.72	11.88	1.570592874	13.45059287	23.49
8	1.447645	7760.824	10.009	1.570603048	11.57960305	22.35
9	1.338871	8391.336	9.53	1.570617571	11.10061757	20.76
10	1.234815	9098.464	5.7	1.570631464	7.270631464	18.84
11	1.157629	9705.112	4.91	1.570641769	6.480641769	16.74
12	1.088729	10319.296	3.97	1.570650968	5.540650968	14.72
13	1.027334	10935.992	1.93	1.570659165	3.500659165	12.65
14	1	11234.92	1.17	1.570662814	2.740662814	10.57

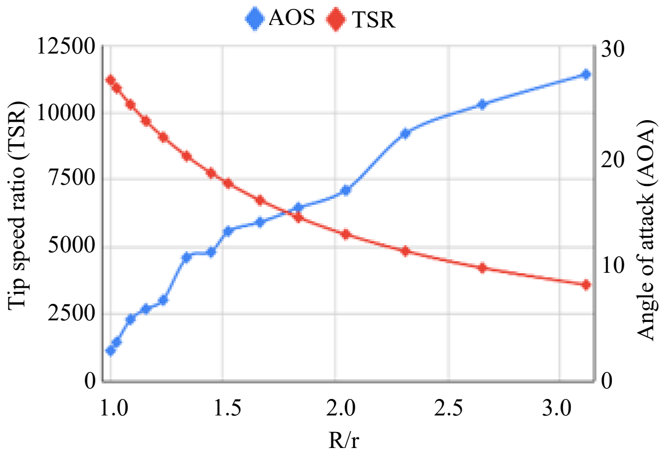

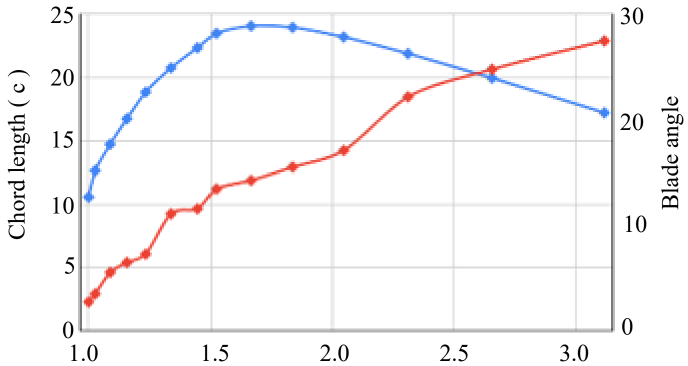

Figure 3. Mathematical parameter for NACA 4412 air foil propeller.

Figure 4. Experimental test setup for static thrust and acoustic analysis.

RESULTS AND DISCUSSION

The aerodynamic and aeroacoustic performance of the UAV propeller was experimentally observed using a controlled laboratory setup, as shown in Figure 4. Thrust measurements were taken at varying motor speeds in RPMs and recorded in grams, after which they were converted to Newtons using standard conversion methods. SPL (dB) were recorded in two controlled indoor laboratory environments (L1 and L2), which were characterized by low ambient noise levels. Thrust and sound levels were analysed simultaneously to evaluate propeller efficiency and noise characteristics across different operating speeds.

For a comprehensive acoustic assessment, the test setup was positioned at varying heights (H1, H2, H3) above the ground. The CESVA SC-260 Class 2 sound level meter (SLM) was placed at distinct positions: X1 meters above the setup at an angle θ_1°, and X2 and X3 meters below. The motor speed was modulated using a remote transmitter, and sound emissions were recorded continuously for 1–2 minutes. Equivalent Continuous Sound Pressure Level (LAT) values were used for graphical representation and analysis.

The graphical illustration in Figure 5 validates that propeller thrust increases proportionally with motor speed, confirming the expected relationship between RPM and lift generation. As the speed of the motor increases with throttle, the airflow over the propeller blades increases, resulting in greater thrust production. Figure 6 illustrates the sound pressure levels at various RPMs, highlighting that propeller noise dominates the overall acoustic profile. The investigation reveals that as the motor speed increases, the sound make by the UAV propeller significantly outweighs the motor noise, emphasizing the need for aeroacoustics optimizations in UAV propeller design to minimize sound emissions while maintaining efficiency.

CONCLUSION

In conclusion, this study presents the mathematical modeling and experimental analysis of a UAV propeller fabricated from PLA material using additive manufacturing (FDM). The propeller, designed using the NACA 4412 airfoil, serves as a baseline configuration to assess aerodynamic and aeroacoustics performance. The results demonstrate that the propeller generates sufficient thrust to support the endurance of the UAV, particularly for indoor flight applications such as filming, photography, and small-scale product delivery.

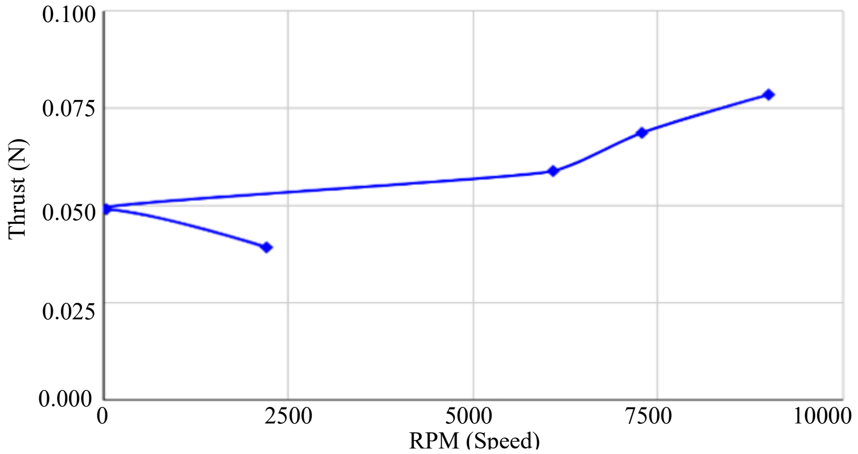

Figure 5. Thrust variation with speed.

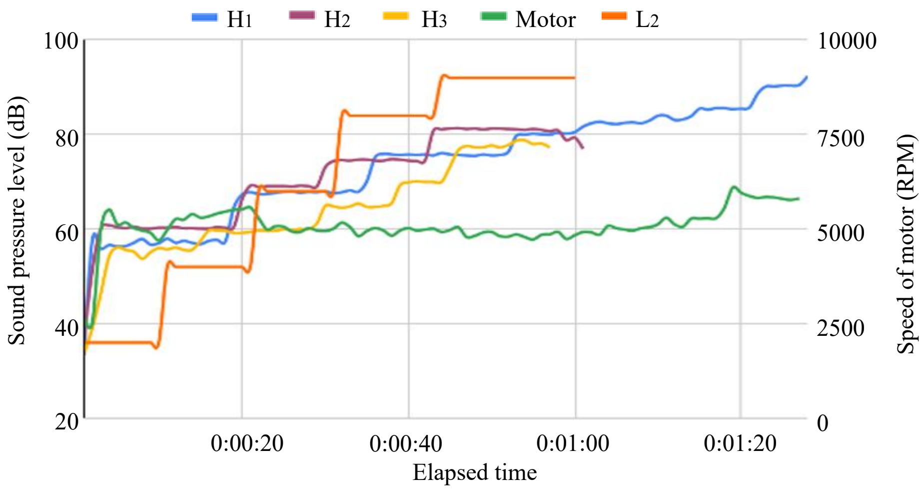

Figure 6. Sound pressure levels with increasing speed and time.

Experimental evaluation revealed variations in sound pressure levels (SPL) and dominant acoustic harmonics at different spatial locations relative to the propeller, offering valuable insights into its noise characteristics. The analysis highlights the relationship between propeller geometry, thrust generation, and acoustic behaviour. To further reduce noise while maximizing thrust, future research will focus on optimizing propeller geometry through variations in blade shape and size. Enhancing endurance and overall efficiency will also remain a key objective. The modelling approach presented in this work contributes to the development of efficient propeller designs that deliver favourable aerodynamic performance while addressing acoustic concerns. Furthermore, propeller designs that incorporate trailing-edge serrations, leading-edge serrations, or looped blade shapes may help enhance aerodynamic efficiency and reduce noise.

Despite these advancements, the sound level of UAV propellers remains a significant challenge, influenced by the complex dynamics of their blades.

Declaration of Interest

"The authors declare that there is no conflict of interest related to the publication of this manuscript."

REFERENCES

1. Cuerno-Rejado, C., Garcia-Hernandez, L., Sanchez-Carmona, A., Carrio, A., SANCHEZ LOPEZ, J. L., & Campoy, P. (2016). Historical evolution of the unmanned aerial vehicles to the present. Dyna, 91(3).

2. Mubina Shekh, S. Rani, and R. Datta, “Review on design, development, and implementation of an unmanned aerial vehicle for various applications,” Int. J. Intell. Robot. Appl., 2024, doi: 10.1007/s41315-024-00359-6.
3. N. Elmeseiry, N. Alshaer, and T. Ismail, “A detailed survey and future directions of unmanned aerial vehicles (UAVs) with potential applications,” Aerospace, vol. 8, no. 12, pp. 1–29, 2021, doi: 10.3390/aerospace8120363.
4. L. Brooke-Holland, “Unmanned Aerial Vehicles (drones): an introduction,” UK House Commons Libr. Stand. Note, p. 21, 2012, [Online]. Available: https://fas.org/irp/world/uk/drones.pdf
5. J. B. McDevitt and A. F. Okuno, “Static and Dynamic Pressure Measurements on a Naca 0012 Airfoil in the Ames High Reynolds Number Facility.,” NASA Tech. Pap., no. June, 1985.
6. P. Shin and K. Kim, “Aerodynamic performance prediction of SG6043 airfoil for a horizontal-axis small wind turbine,” J. Phys. Conf. Ser., vol. 1452, no. 1, 2020, doi: 10.1088/1742-6596/1452/1/012018.
7. R. K. Singh, M. R. Ahmed, M. A. Zullah, and Y. H. Lee, “Design of a low Reynolds number airfoil for small horizontal axis wind turbines,” Renew. Energy, vol. 42, pp. 66–76, 2012, doi: 10.1016/j.renene.2011.09.014.
8. T. Ganesan and N. Jayarajan, “Aerodynamic Analysis of Mathematically Modelled Propeller for Small UAV Using CFD in Different Temperature Conditions,” Stroj. Vestnik/Journal Mech. Eng., vol. 69, no. 11–12, pp. 444–454, 2023, doi: 10.5545/sv-jme.2023.601.
9. R. Benmounah and A. Merabet, “A numerical study of the aerodynamic flow around a UAV propeller with a naca 4412 type blade airfoil,” AIP Conf. Proc., vol. 2415, no. December, 2022, doi: 10.1063/5.0092283.
10. N. S. Zawodny and D. D. Boyd, “Investigation of rotor–airframe interaction noise associated with small-scale rotary-wing unmanned aircraft systems,” J. Am. Helicopter Soc., vol. 65, no. 1, 2020, doi: 10.4050/JAHS.65.012007.
11. X.-D. Vu, A.-T. Nguyen, T.-L. Nha, H.-Q. Chu, and C.-T. Dinh, “Numerical Aerodynamic and Aeroacoustic Analysis of Toroidal Propeller Designs,” Int. J. Aviat. Sci. Technol., vol. vm05, no. is01, pp. 20–33, 2024, doi: 10.23890/ijast.vm05is01.0102.
12. Y. Gu et al., “Numerical and experimental studies on the owl-inspired propellers with various serrated trailing edges,” Appl. Acoust., vol. 220, no. March, p. 109948, 2024, doi: 10.1016/j.apacoust.2024.109948.
13. M. A. Chakchouk, A. El Hami, P. R. Dahoo, A. Lakhlifi, W. Gafsi, and M. Haddar, “The impact of curved-tip propeller geometry on hovering drone performance for air quality monitoring,” Adv. Mech. Eng., vol. 15, no. 10, 2023, doi: 10.1177/16878132231206330.
14. Van Treuren, K. W., & Hays, A. W. (2017). A study of noise generation on the e387, s823, NACA 0012, and NACA 4412 airfoils for use on small-scale wind turbines in the urban environment. Journal of Energy Resources Technology, 139(5), 051217.
15. Hanson, L. P., Baskaran, K., Pullin, S. F., Zhou, B. Y., Zang, B., & Azarpeyvand, M. (2022). Aeroacoustic and aerodynamic characteristics of propeller tip geometries. In 28th AIAA/CEAS Aeroacoustics 2022 Conference (p. 3075).
16. MacNeill, R., & Verstraete, D. (2017). Blade element momentum theory extended to model low Reynolds number propeller performance. The Aeronautical Journal, 121(1240), 835–857.
17. Oliveira, N. L., Rendón, M. A., Lemonge, A. C. D. C., & Hallak, P. H. (2024). Multi-objective optimum design of propellers using the blade element theory and evolutionary algorithms. Evolutionary Intelligence, 17(3), 1623–1653.
18. Fontana, L., Minetola, P., Iuliano, L., Rifuggiato, S., Khandpur, M. S., & Stiuso, V. (2022). An investigation of the influence of 3d printing parameters on the tensile strength of PLA material. Materials Today: Proceedings, 57, 657–663.
19. Raj, S. A., Muthukumaran, E., & Jayakrishna, K. (2018). A case study of 3D printed PLA and its mechanical properties. Materials Today: Proceedings, 5(5), 11219–11226.
20. Ansari, A. K., & Kumar, P. (2024). Vibration and acoustics analyses of tapered roller bearing. Journal of Vibration Engineering & Technologies, 12(2), 2467–2484.

